Materials Today Bio 24 (2024) 100910

Contents lists available at ScienceDirect

Materials Today Bio

journal homepage: www.journals.elsevier.com/materials-today-bio

The mechanism of adipose mesenchymal stem cells to stabilize the immune microenvironment of pelvic floor injury by regulating pyroptosis and promoting tissue repair

Xiaotong Wu [a,b,1], Fengshi Zhang [c,1], Xiaolin Mao [d,1], Fujian Xu [d], Xiaokang Ding [d,***], Xiuli Sun [a,b,**], Jianliu Wang [a,b,*]

[a] Department of Obstetrics and Gynecology, Peking University People's Hospital, 100044, Beijing, China
[b] Beijing Key Laboratory of Female Pelvic Floor Disorders, 100044, Beijing, China
[c] Department of Orthopedics and Trauma, Peking University People's Hospital, 100044, Beijing, China
[d] College of Materials Science and Engineering, Beijing University of Chemical Technology, 100029, Beijing, China

ARTICLE INFO

Keywords:
Mechanical force
Pyroptosis
ADSCs
Immune regulation
Antioxidant

ABSTRACT

Pelvic organ prolapse (POP) has a high incidence rate among Chinese women. Repeated mechanical stimulation is an important factor causing POP, but the injury mechanism has not yet been elucidated. The purpose of this study is to explore the related mechanisms of pelvic floor supporting tissue damage caused by mechanical force and the application of stem cell therapy. First, we obtained vaginal wall and sacral ligament tissue samples from clinical patients for examination. Pelvic floor support tissues of POP patients displayed high expression of inflammation and immune disorders. Then, we constructed a rat model of childbirth injury. In vivo and in vitro experiments investigated the key mechanism of pelvic floor support tissue injury caused by mechanical force. We discovered that after mechanical force, a large number of reactive oxygen species (ROS) and macrophages rapidly accumulated in pelvic floor tissues. ROS stimulated macrophages to produce NLRP3 inflammatory complex, induced the release of interleukin (IL-1β) and pyroptosis and exacerbated the inflammatory state of damaged tissues, persisting chronic inflammation of fibroblasts in supporting tissues, thus causing the pelvic floor's extracellular matrix (ECM) collagen metabolic disorder. Resultingly impeding the repair process, thereby causing the onset and progression of the disease. Through their paracrine ability, we discovered that adipose mesenchymal stem cells (ADSCs) could inhibit this series of pathological processes and promote tissue repair, asserting a good therapeutic effect. Simultaneously, to overcome the low cell survival rate and poor therapeutic effect of directly injecting cells, we developed a ROS-responsive PVA@COLI hydrogel with ADSCs. The ROS-scavenging properties of the gel could reshape the site of inflammation injury, enhance cell survival, and play a role in subsequent treatment. The findings of this study could serve as a basis for early, targeted intervention therapy for POP and representing a promising approach.

1. Translational impact statement

The effect of mechanical force on the microenvironment of pelvic floor tissue, which leads to the occurrence and development of diseases, has not been given enough attention. This study investigated the key mechanism underlying the mechanical force-induced damage to the pelvic floor support structure and innovatively proposed that the relationship between tissue mechanical force, inflammation, immunity, and tissue damage may be the key mechanism mediating the onset of pelvic organ prolapse (POP).

2. Introduction

The incidence of pelvic organ prolapses (POP) among Chinese adult

* Corresponding author. Department of Obstetrics and Gynecology, Peking University People's Hospital, 100044, Beijing, China.
** Corresponding author. Beijing Key Laboratory of Female Pelvic Floor Disorders, 100044, Beijing, China.
*** Corresponding author.
1 These authors contributed equally.
E-mail addresses: dingxk@mail.buct.edu.cn (X. Ding), sunxiuli@pkuph.edu.cn (X. Sun), wangjianliu@pkuph.edu.cn (J. Wang).

https://doi.org/10.1016/j.mtbio.2023.100910
Received 26 July 2023; Received in revised form 19 November 2023; Accepted 9 December 2023
Available online 18 December 2023

women has reached 9.6 % [1]. Multiple factors contributed to the progressive deterioration of the pelvic floor support structure, negatively impacting the patient's quality of life. Pregnancy, childbirth and vaginal dystocia are independent high-risk factors for POP. The connective tissues of the pelvic floor consist of fascia and ligaments, with extracellular matrix (ECM) secreted primarily by fibroblasts as its main component [2,3]. ECM degradation can result from repeated mechanical stimulation over time [4,5]. Single-cell sequencing of the vaginal wall based on normal population and POP patients revealed that abnormal ECM regulation and immune disorders had an imperative role in the POP occurrence [6]. Consequently, it is crucial in preventing POP to investigate the primary mechanism of pelvic floor support tissue injury caused by mechanical force, to carry out accurate early intervention according to the key targets, and to delay and prevent the disease's development with safer and more effective treatment methods.

Mechanical forces at the level of injury will result in a metabolic imbalance of the antioxidant system, and the reactive oxygen species (ROS) produced by this imbalance can cause irreversible damage to the pelvic floor supporting tissues [7]. Immune cells, particularly monocytes and macrophages, will migrate to the injured site to remove necrotic cells and for tissue repair and regeneration. As a fundamental component of innate immunity, macrophages play a vital part in homeostasis and inflammatory diseases in vivo [8]. The immune regulation of macrophages is divided depending on their phenotype and function: classically activated macrophages (M1) and alternately activated macrophages (M2). M1 macrophages are the first to appear at the injury site, secreting inflammatory cytokines such as interleukin (IL-1β), tumor necrosis factor α (TNF-α), IL-6, and matrix metalloproteinase (MMP-1), involved in necrotic tissue clearance and ECM degradation. M2-type macrophages secrete anti-inflammatory cytokines, including IL-4, IL-10, and transforming growth factor (TGF)-β, involved in matrix synthesis [9] and promotion of tissue regeneration. Different macrophage phenotypes serve distinct functions in diverse microenvironments. This differentiation is known as macrophage polarization, and the balance of macrophage polarization closely relates to tissue inflammatory response. ROS accumulation can activate macrophages to produce inflammatory bodies [10]. The production of active caspase-1 is stimulated by the activation of the inflammatory body NLRP3, bringing about two major effects: the maturation and secretion of the cellular inflammatory cytokine IL-1β, IL-18 and pyroptosis [11]. IL-1β is a potent inflammatory factor that can upregulate MMP production, promote ECM degradation, and cause severe inflammatory injury [12]. Following pyroptosis, cell membrane perforation releases numerous inflammatory factors, resulting in persistent chronic inflammation and the imbalance of the immune microenvironment, which participates in the pathological processes of various diseases [13]. The research and mechanism of pelvic floor support tissue injury due to mechanical force have not been reported.

Literature studies have demonstrated that implantation of stem cells in vivo can enhance the function of target organs as stem cells could potentially repair and regenerate [14,15]. Mesenchymal stem cells (MSCs) have garnered considerable interest as adult stem cells; they can undergo autologous transplantation, are ethically and legally unrestricted, and overcome other adverse effects such as genetic mutations. Common MSCs include bone marrow MSCs (BMSCs), endometrial MSCs (EMSCs) and adipose MSCs (ADSCs). Studies have shown that adipose tissue is abundant and relatively easy to obtain, and ADSCs have a greater proliferative and paracrine capacity than BMSCs; therefore, ADSCs are beneficial for cell therapy [16]. Currently, research on the repair mechanism of stem cells for POP is limited, but evidence suggests that the paracrine effect of stem cells may be the primary reason for its remarkable therapeutic effect [17]. Recently, a newly proposed mechanism of action for the paracrine ability of stem cells is antioxidant capacity [18]. As stated, MSCs decrease ROS production, improving the antioxidant capacity of cells and tissues, reducing the response of cells to inflammation and oxidation [19], and diminishing inflammatory factors at the site of injury, thus, protecting and repairing the damaged tissues [20].

Following tissue injury, the microenvironment is unfavorable for stem cells' survival in local treatment and the subsequent therapeutic effect. With the advent of tissue engineering biomaterials, numerous new biomaterials and therapeutic methods have emerged. Hydrogels are injectable biomaterials that deliver biological entities such as cells and exosomes with high biocompatibility and physicochemical properties similar to human tissues. This study prepared a ROS-responsive collagen hydrogel cell carrier for local injection to deliver ADSCs to the injured tissue site accurately. Moreover, in an inflammatory environment with high ROS levels, the hydrogel scaffold could gradually release stem cells while consuming ROS, playing a sustained therapeutic role.

Consequently, this study investigated the primary mechanism of pelvic floor support structure damage caused by mechanical force such as vaginal delivery, combined with an innovative hydrogel cell delivery system to determine the effect and mechanism of ADSCs in repairing damaged pelvic floor support tissue.

3. Materials and methods

3.1. Clinical case data selection and histological staining

Three POP patients diagnosed as stage III and IV and who had undergone pelvic floor reconstruction surgery at the Obstetrics and Gynecology of Peking University People's Hospital were included. Three donor tissues from patients undergoing hysterectomy for non-POP conditions were chosen as a control group. Expert physicians removed samples of the uterine sacral ligament and vaginal wall which were immediately frozen for preservation. The study was conducted under the Ethics Committee of Peking University People's Hospital (2021PHB137-001). Furthermore, all samples were obtained from the Peking University People's Hospital Biobank and gathered for further examination. H&E staining was done to assess the morphology.

3.1.1. Immunohistochemistry assessment

To measure the impact of pyroptosis on POP, the uterine sacral ligament and vaginal wall were fixed in paraformaldehyde at 4 °C and incubated with the following primary antibodies overnight at 4 °C: anti-NLRP3 (1:400, NOVUS). After washing thrice with PBS, slides were incubated with secondary antibodies conjugated to Alexa fluor 488 (1:800, Invitrogen) at 37 °C for 1 h. The nuclei were labeled with DAPI, and fluorescent images were observed through a microscope.

3.2. Animal studies

A total of 57 Sixty female SD rats aged eight weeks (205 ± 15 g) were provided by the laboratory animal unit of Peking University People's Hospital, Beijing, China. The animal study was conducted according to the Ethics Committee on Animals of Peking University People's Hospital (2022PHE085). Animal experiments were conducted in an environment free of specific pathogens. The rats were placed in a temperature-controlled chamber with relative humidity between 50 and 60 % and a 12 h light/dark cycle. The animals had free access to food and water throughout the experiment.

3.2.1. Animal modeling methods

Following the administration of 2.5 % isoflurane (RWD, Shenzhen, China) using an animal anesthesia machine (RWD, Shenzhen, China). , SPF female SD rats aged eight weeks were fixed with the vagina exposed. Additionally, an F10 catheter was inserted vaginally, and 3 ml saline was injected into the balloon. The pubic union was placed at the table margin to maintain 130 g sagging tension for 2 h. After modeling, ADSCs were injected in situ in the ADSCs treatment group. After the surgery, the rats were administered pain-preventing jelly (NEWLOONG LIFE SCIETECH, Shanghai, China). Daily, the animals were closely monitored. All

measures were taken to reduce animal suffering. The rats were sacrificed for subsequent experiments after four days of operation.

3.2.2. Grouping of experimental animals

Experimental animals were separated into three groups, control groups, experimental groups and ADSCs treatment groups (n = 5); with a vaginal balloon inserted and the control group with no balloon dilation or distal gravity pulling.

3.2.3. The in vivo fluorescence imaging

Col/ADSCs and Gel/ADSCs were injected into the modeling rats at each time point (n = 3). The collagen concentration was 2 mg/ml, and the density of ADSCs was 10^7/ml. Multiple injections were administered to the vaginal wall of the rats, and luciferin substrate was injected 10 min prior to imaging.

3.2.4. Histological staining

The rats were euthanized four days after the injection, and the vaginal walls were attained for analysis. The samples were fixed with paraformaldehyde for 24 h, dehydrated in an alcohol gradient, and placed on a paraffin slicer for sectioning. The slices were approximately 3–4 μm thick, numbered, and placed in a 60 °C oven for baking. H&E, Masson's trichrome and Sirius Red staining were performed according to the instructions described previously [21].

3.3. Cell pyroptosis assay

ADSCs were cultured, isolated, differentiated, identified, and transfected with fluorescence as previously done, and passage numbers below 10 were used in the study [22]. Fibroblast cell line FB and macrophage cell line J774A.1 were obtained from Procell Life Science & Technology, Wuhan, China. Furthermore, LPS 1 μg/ml was used to stimulate J774A.1 for 4 h, and 5 μM nigericin was added for 1 h to induce pyroptosis in vitro. The ADSCs treatment group was substituted and co-cultured with stem cells for 24 h.

3.4. Caspase-1 activity assay

The caspase-1 activity was detected via the caspase-1 activity assay kit (Beyotime, China) following the manufacturer's instructions. This assay kit is based on the ability of caspase-1 to catalyze the substrate acetyl-Tyr-Val-Ala-Asp *p*-nitroanilide (Ac-YVAD pNA) to produce yellow *p*-nitroaniline (pNA), which has a strong absorption at 405 nm. Consequently, the activity of caspase-1 can be evaluated by measuring the absorbance of pNA utilizing a standard pNA curve.

3.5. Lactate dehydrogenase (LDH) activity assay

The extent of intracellular injury in pyroptotic cell death was analyzed via LDH activity in a culture medium using a colorimetric assay kit (Jiancheng, Nanjing, China) according to the manufacturer's instructions. The results were compared with the total LDH released from the cells.

3.6. Western blot

Cells or tissues homogenate were lysed by Ripa lysis buffer (KeyGEN Bio TECH) containing protease and phosphatase inhibitors. The extracted proteins were quantified using BCA Protein Assay Kit (Thermo Scientific) and WB analysis of MMP1 (1:1000, Proteintech), MMP9 (1:1000, Proteintech), TIMP1 (1:1000, Proteintech), COL1A1 (1:1000, CST), COL3A1 (1:1000, Santa), NLRP3 (1:1000, NOVUS), N-GSDMD (1:1000, Affinity), Caspase1 (1:1000, CST), IL-1β (1:1000, Affinity), iNOS (1:1000, Proteintech), Arg-1 (1:1000, CST), SOD (1:1000, Proteintech) and GSH were conducted following the standard methods provided by Cell Signaling Technology and quantified using Image J software.

3.7. Flow cytometry assessment

3.7.1. Flow cytometry detected the cell surface marker

The cells were prepared and collected in EP tubes via centrifugation. PBS was utilized for cell suspension, followed by adding 3–5 μL of target antibody per 100 μL, incubated at room temperature for 30 min and washed with 300 g of PBS thrice. The final results were detected using a BD FACS CantoII machine and analyzed using Flow jo.

3.7.2. Flow cytometry detected caspase-1 expression

The caspase-1 activity assay kit (Immuno Chemistry, Technologies, LLC) was used per the manufacturer's instructions to detect the caspase-1 activity. This assay kit is an active caspase enzyme inside the cell; it covalently binds with FLICA and retains the green fluorescent signal within the cell. FLICA diffuses out of the cell during the wash steps if unbound. Pyroptotic cells containing a higher concentration of FLICA emit a brighter fluorescence than healthy cells.

3.7.3. The ROS scavenging assay

The ROS was detected using the ROS assay kit -Highly Sensitive DCFH-DA (Dojindo, Japan). In an animal model, the mucous layer of the vaginal wall was selected and isolated into a single-cell suspension. The cell concentration was adjusted from 1×10^6 to 2×10^7/ml. Moreover, the cells were re-suspended in the diluted DCFH-DA, incubated at 37 °C for 30 min, washed thrice with PBS and detected by flow cytometry.

3.8. Immunofluorescence analysis

The prepared cells were fixed in 4 % paraformaldehyde for 15 min, incubated with PBS containing Triton-100x for 10 min and BSA for 1 h. Following the incubation with the primary antibody (anti-caspase-1, anti-NLRP3, anti-ASC and anti-Ki67, 1:200) at 4 °C overnight, the corresponding secondary antibody was added to the cells and incubated at 37 °C for 1 h. Nuclei were stained with DAPI before imaging and captured using a microscope (Leica).

3.9. Preparation and characterization of hydrogels

The ROS-responsive crosslinker TSPBA was synthesized via a quaternization reaction of *N,N,N′,N′*-tetramethyl-1,3-propanediamine and 4-(bromomethyl) phenylboronic acid [23], and its structure was confirmed by ^{1}H NMR. Hydrogels were prepared by the crosslinking of PVA 1788 (8 wt%), TSPBA (10 wt%) and collagen (2 mg/mL) with the volume ratio of 5:2:3, and the crosslinking time was about 50 min. The microstructure morphologies of freeze-dried hydrogels were observed by scanning electron microscopy (SEM). The injectability and self-healing properties of hydrogels were measured via a rheometer. The ROS responsiveness of hydrogels was proved with 20 mM H_2O_2, and free radical scavenging performance was verified by 0.1 mM DPPH. The ROS scavenging performance of the hydrogels was confirmed with 20 mM of H_2O_2 and 0.1 mM of DPPH, respectively.

3.10. Biocompatibility of gel

3.10.1. CCK8

The configured gel should cover the bottom of the 96-well plate completely and then be co-cultured with ADSCs. Ten microliters of CCK8 solution (Dojindo, Japan) were added to each well and incubated at 37 °C for 96 h, four wells from each group were collected for analysis.

3.10.2. EdU

The configured gel should cover the bottom of the 96-well plate completely. It was co-cultured with ADSCs. The EdU was detected using an EdU assay kit (Ribo, China) as specified by the manufacturer. EdU is a

thymidine nucleoside analog that can infiltrate the DNA molecule to be synthesized, replacing thymine (T) during DNA replication. On the basis of a specific reaction between Apollo® fluorescent dye and EdU, DNA replication activity can be detected directly and precisely.

3.10.3. Live-dead cell staining

The configured gel to cover the bottom of the six-well plate completely and co-cultured with ADSCs. The live/dead staining was assessed via Calcein-AM/PI double staining kit (Dojindo, Japan) according to the manufacturer's instructions. Calcein-AM penetrates the cell membrane, emitting strong green fluorescence. Therefore, green fluorescence is detectable in living cells. PI enters the dead cell through the damaged cell membrane and embeds in the DNA double helix of the cell to produce red fluorescence, so red fluorescence is detectable in dead cells.

3.11. Statistical analysis

All results were presented as the mean ± standard deviation (SD). Unpaired Student's t-test was utilized for the direct comparison between the two groups. One-way analysis of variance (ANOVA) with the Newman-Keuls posttest was employed to compare the means of three or more groups. *$P < 0.05$; **$P < 0.01$; ***$P < 0.001$; n. s., not significant ($P > 0.05$).

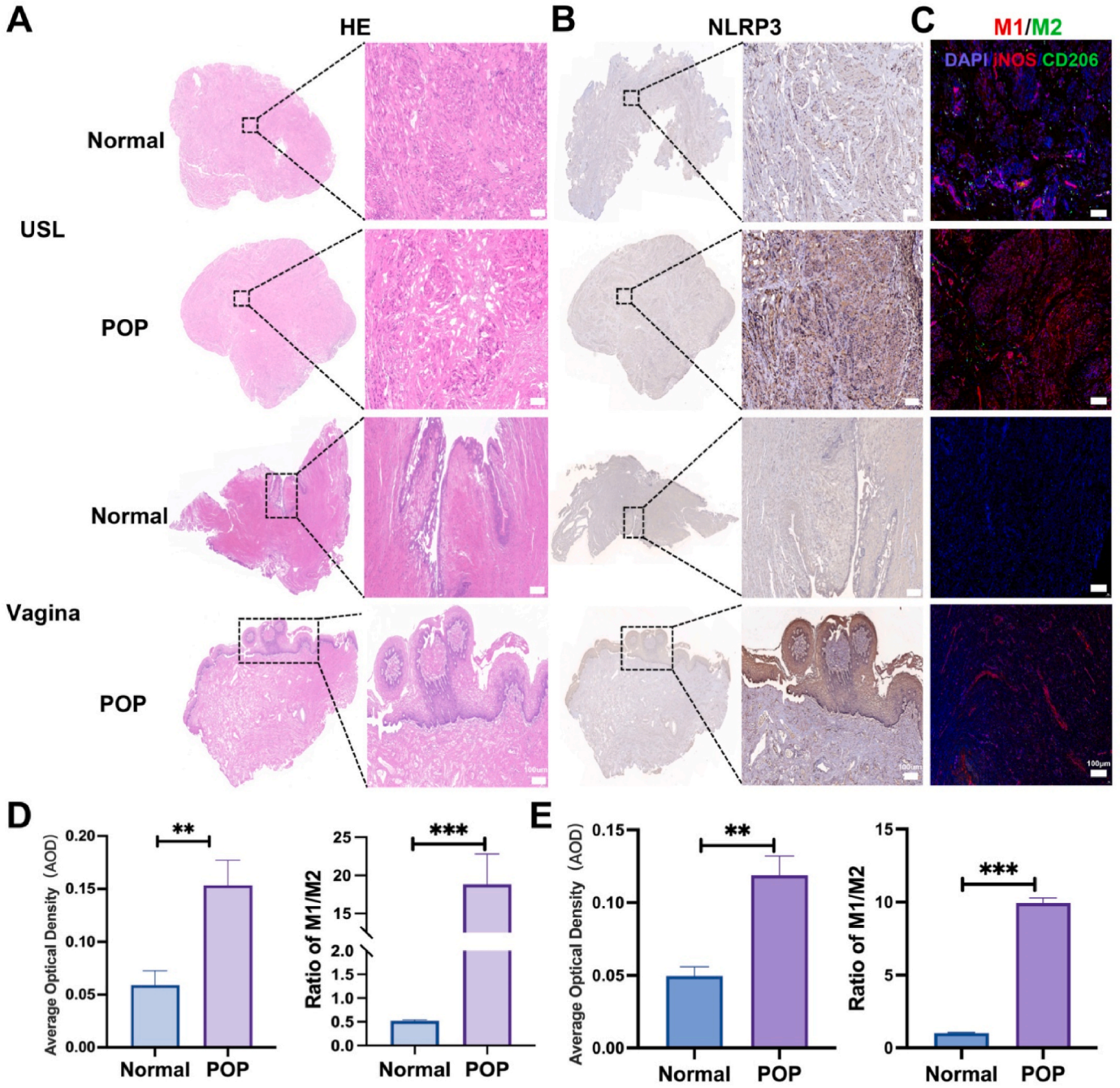

Fig. 1. Inflammation and immune disorders could be the molecular basis of POP. (A–C) H&E staining, IHC staining and immunofluorescence of NLRP3, iNOS, CD206 in USL and vagina wall. Scale bar: 100 μm. (D–E) Analysis of average optical density and the ratio of M1/M2 macrophages in the USL and vaginal wall. Values are expressed as mean ± SD (n = 3). Statistical analysis was performed by the unpaired *t*-test. **$P < 0.01$, ***$P < 0.001$. USL, Uterosacral ligaments.

4. Results

4.1. Dysregulation of inflammation and immune microenvironment existed in POP patients

The pelvic floor support tissues of POP-Q stage III and IV patients, sacral ligament and vaginal wall tissues, were collected for the H&E staining. Compared to the connective tissue structure of normal people, the collagen arrangement was disordered and loose (Fig. 1A). Immunohistochemical staining revealed a significant increase in NLRP3 expression in the pelvic floor support tissues of POP patients (Fig. 1B). In POP patients' diseased tissues, an inflammatory response and pyroptosis was existed. Immunofluorescence staining also disclosed macrophage imbalance (Fig. 1C); significant statistical differences were observed in the immune microenvironment of the supporting tissues of the pelvic floor in patients (Fig. 1D and E). We speculated that the disorder of inflammation and immune microenvironment might be the basis and key to the occurrence and development of POP disease.

4.2. ADSCs can alleviate mechanical force-induced vaginal wall injury in rats

The rat model of delivery injury was constructed using the balloon dilation method. The modeling process and sampling time point are shown in Fig. 2B. After mechanical force action, the vaginal hiatus increased, and the perineal body was slightly abnormal. H&E staining was used to examine the tissue and cell morphology at the sampling site. The results revealed a thinner vaginal wall in the vaginal dilatation (VD) group upon laceration. The normal structure of the vaginal wall was restored to a certain extent in the ADSCs treatment group. Masson

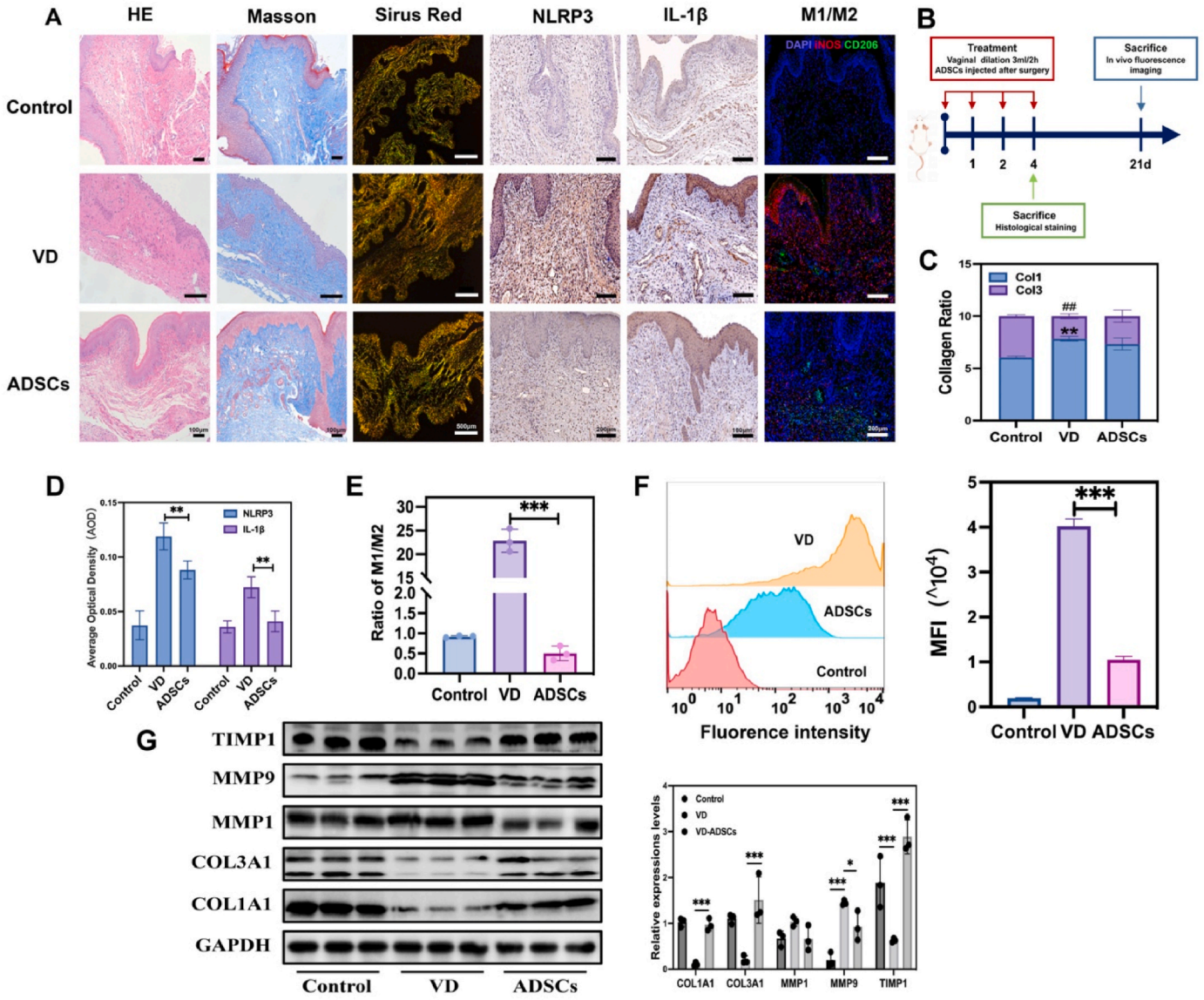

Fig. 2. ADSCs have a therapeutic effect on collagen ratio after mechanical injury. (A) H&E, Masson, Sirius Red staining, IHC staining and immunofluorescence of NLRP3, IL-1β, iNOS, CD206 in the rat vagina wall. Scale bar: 100 μm. (B) Plots of the schedule in rat preclinical model. (C) Analysis of collagen I/III ratio, values are expressed as mean ± SD (n = 5), one-way ANOVA, * means collagen I statistically significant difference compared with the control group, # means collagen III statistically significant difference compared with the sham operation group, P < 0.01. (D–E) Analysis of average optical density of NLRP3, IL-1β and ratio of M1/M2 macrophages in the vaginal wall, values are expressed as mean ± SD (n = 5), one-way ANOVA, *$P < 0.05$, **$P < 0.01$, ***$P < 0.001$. (F) The ROS accumulation at the injured vaginal wall and the antioxidant capacity of ADSCs were studied by flow cytometry. Statistics analysis was performed using one-way ANOVA. ***$P < 0.001$. (G) Immunoblots for expression of COL1A1, COL3A1, MMP1, MMP9 and TIMP1 in the rat vaginal wall tissue, values are expressed as mean ± SD (n = 5), one-way ANOVA, *$P < 0.05$, **$P < 0.01$, ***$P < 0.001$. VD, vaginal dilatation and ROS, reactive oxygen species.

staining distinguishes collagen fibers from muscle fibers in tissues; muscle fibers and red blood cells are dyed red, while collagen fibers, cartilage and mucus are stained blue. According to the findings, rats in the VD group had thinner cortical layers of the vaginal wall, disorganized collagen arrangement, and partially broken muscle fibers. Furthermore, the cortical layer of the vaginal wall partially recovered, and collagen production was increased in the rats of the ADSCs group; however, the distribution was loose. In Sirius Red staining, different collagen fibers reflect distinct colors under polarized light to distinguish collagen types. Type I collagen is red or yellow, and type III collagen is green. In the control group, type I and type III collagen were staggered to form the connective tissue of the vaginal wall. In the VD group, the distribution of the type I collagen was increased, type III collagen was reduced, and the proportion of type I/III collagen was unbalanced. The ADSCs group had an increased amount of new type III collagen. Type I collagen fibers are coarse, mainly providing tissue tension and enhancing the toughness of ligament-connective tissue. Type III collagen is thinner and more elastic, primarily maintaining tissue elasticity; the proportion of type I/III collagen influences the tissue's strength and elasticity after healing (Fig. 2A). Moreover, we analyzed the proportion of collagen types in each group following the injury (Fig. 2C). The results found the highest ratio of type I collagen in the VD group ($P < 0.01$), while the proportion of type III collagen was the lowest ($P < 0.01$). In the ADSCs treatment group, type III collagen was largely repaired, indicating that ADSCs may enhance the elasticity of regenerated tissue following damage repair; nonetheless, no significant statistical difference was found between the two groups ($P > 0.05$).

4.3. ADSCs can relieve focal death of pelvic floor support tissue, immune imbalance and ECM metabolism disorder caused by mechanical force

According to studies, mechanical force at the level of injury leads to the metabolic imbalance of the body's antioxidants, and ROS produced by this imbalance can cause irreversible damage to pelvic floor-supporting tissues [7]. In this research, ROS detected in the vaginal wall tissues of each group indicated significant ROS accumulation in the VD group and decreased build up in the ADSCs group (Fig. 2F). Simultaneously, ECM in the vaginal wall of animal models exposed that mechanical force injury could result in the metabolic disorder of ECM (Fig. 2G), which showed that the synthesis of COL1A1, COL3A1 and TIMP1 promoting collagen synthesis decreased, while the MMP9 degrading collagen increased. Thus, ADSCs can alleviate ROS accumulation and ECM metabolism abnormalities to some extent.

Extensive research confirms that excessive ROS accumulation resulting from a mechanical injury is crucial in activating M1-type macrophages to produce inflammatory bodies, NLRP3 [10]. Activated NLRP3 has two major effects: maturation and secretion of the cellular inflammatory cytokines, IL-1β and IL-18 and pyroptosis [24]. IL-1β is a potent inflammatory factor that can upregulate MMP production, promote ECM degradation, and cause severe inflammatory injury [25]. Immunohistochemical findings demonstrated that the expressions of NLRP3 and IL-1β were significantly increased in the vaginal wall tissues of the VD group, and stem cells could reduce tissue inflammation and pyrodeath to a certain extent (Fig. 2A and D, $P < 0.01$).

Following injury, immune cells, particularly monocytes/macrophages, migrate to the site of injury to participate in necrotic cell clearance and tissue repair and regeneration. According to their phenotype and function, the immune regulation of macrophages can be divided into classically activated macrophages (M1) and alternately activated macrophages (M2). Immunofluorescence M1 (iNOS + Red)/M2 (CD206+Green) staining and statistical analysis were performed on the vaginal wall tissues of each group. Under normal conditions, macrophages are in a static state, and in the VD group, following injury, a large number of M1 macrophages and a small number of M2 macrophages were observed, whereas in the ADSCs group, a large number of M2 macrophages were seen. According to the analysis of each group's macrophage proportion, the VD group had M1-type macrophages dominantly ($P < 0.01$), while M2-type macrophages were dominant in the ADSCs group (Fig. 2A and E, $P < 0.01$). Supported by much evidence, ADSCs could induce the polarization of macrophages from M1 to M2 type, promoting the repair of pelvic floor support structure.

4.4. The paracrine capacity of ADSCs plays an important role in the treatment of cell injury

After the injury, ROS accumulation, activation of inflammatory body NLRP3, and pyroptosis were observed in vivo. Additionally, ADSCs played a therapeutic role to a certain extent. Furthermore, in vitro experiments were conducted to determine whether ADSCs could inhibit pyroptosis and thus regulate the immune microenvironment. First, fibroblasts were treated with LPS to simulate cellular inflammatory injury, and ADSCs were co-cultured. Flow cytometry was utilized to determine ADSCs' ability to scavenge ROS, and the results demonstrated that ADSCs can reduce ROS production in fibroblasts following LPS treatment (Fig. 3A, $P < 0.05$). Moreover, the expression of the antioxidant protein in fibroblasts increased after treatment with ADSCs (Fig. 3B, $P < 0.001$). The most recent theory state that free radicals, inflammation, and aging are intimately connected [26]. As a result, LPS-treated fibroblasts were stained with β-galactosidase, and the aging cells produced dark blue products. The findings revealed that fibroblasts were senescent after inflammatory injury, while senescent cells decreased in the ADSCs co-culture group (Fig. 3C). It was speculated that ADSCs could reduce senescence by preventing the oxidative damage to fibroblasts. In addition, we induced pyroptosis of macrophages utilizing LPS in conjunction with nigericin and co-cultured them with ADSCs for intervention. First, Western blot combined with Immunofluorescence disclosed that following the LPS and nigericin, macrophage inflammatory bodies NLRP3, N-GSDMD, IL-1β and caspase-1 (P20) increased to varying degrees, suggesting successful induction of caustic death. However, ADSCs could, to some extent, impede the progression of pyroptosis, and the expression of proteins associated with pyroptosis was reduced (Fig. 3D and E), with a statistically significant difference. LDH is a stable cytoplasmic enzyme present in all cells. When the cell membrane is compromised, the LDH is swiftly released into the cell culture medium. We detected LDH production in each group of cells. ADSCs can mitigate the damage caused by pyroptosis to cells (Fig. 3I).

The classic pyroptosis pathway cleaved caspase-1 and gasdermin D (GSDMD), cleaved the key effect protein, forming the n-terminal domain, recognizing and perforating the cell membrane, resulting in cell swelling and rupture, and cell pyroptosis. Therefore, immunofluorescence and flow cytometry were carried out to assess the cas1 (YVAD) expression and the activity of caspase-1 in cell supernatant to explore the key molecule caspase-1 in pyroptosis and determine if ADSCs can mitigate pyroptosis damage. The findings demonstrated that ADSCs could inhibit the activity of caspase-1 to varying degrees, thereby mitigating the pyroptosis -induced cell damage (Fig. 3G, H, and J). Furthermore, fibroblast stimulation via LPS and nigericin to induce inflammatory injury in vitro exposed that ADSCs could accelerate ECM reconstruction after injury, manifested by increased collagen synthesis and decreased degradation (Fig. 3K). Finally, we co-cultured the stem cells with M1-type macrophages to verify whether the anti-inflammatory regulation of ADSCs plays a role through its immune regulation ability by polarizing macrophages from M1 to M2 and the transition from the injury-inflammatory state to the process of tissue repair. Furthermore, expressions of pro-inflammatory factors IL-1β and IL-6 and anti-inflammatory factors IL-4 and IL-6 were detected (Fig. 3L). The study results highlighted that ADSCs could increase the secretion of anti-inflammatory factors in macrophages and polarize M1 to M2-type macrophages with statistically significant differences (Fig. 3M, N and O).

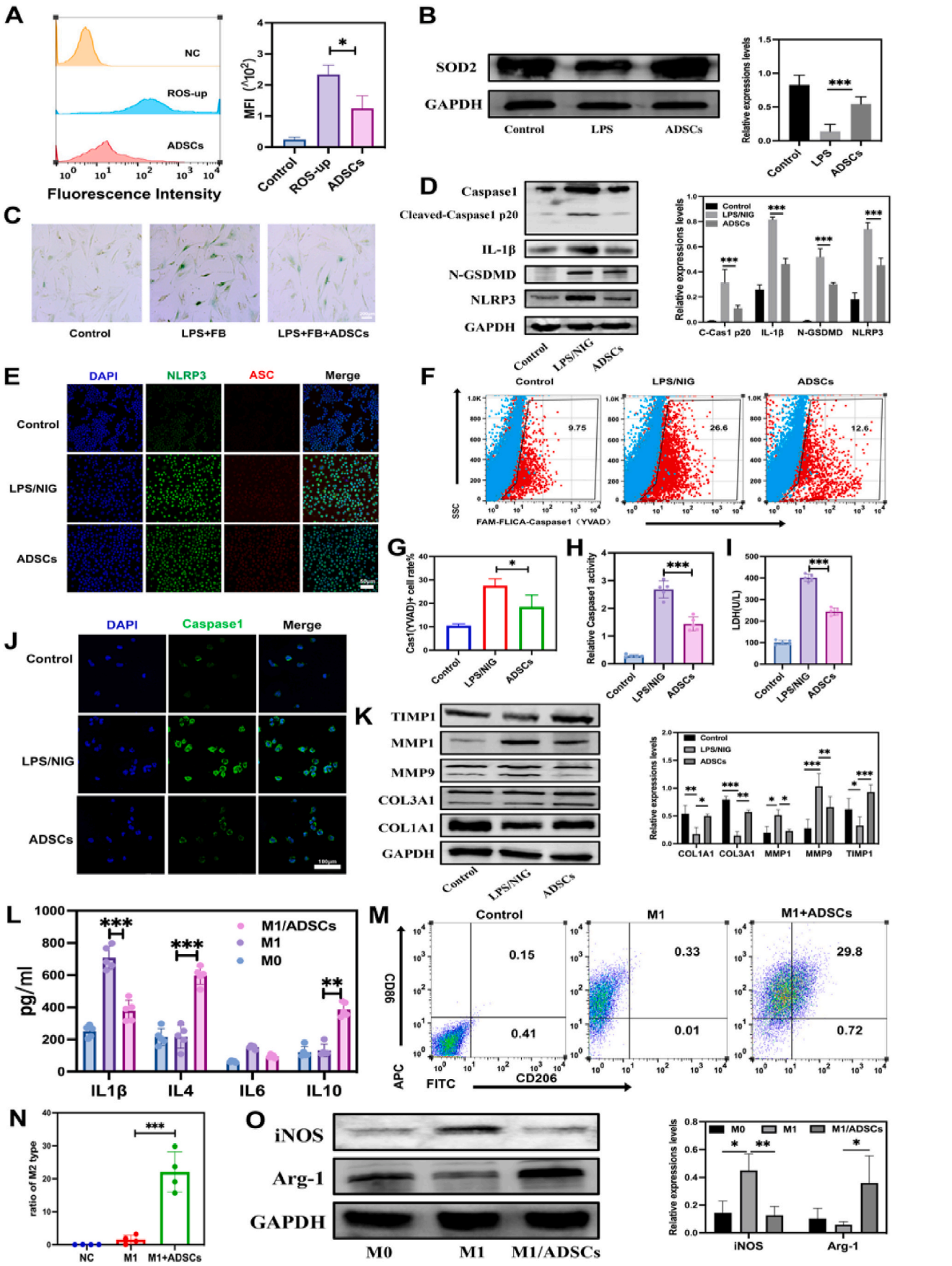

(caption on next page)

Fig. 3. ADSCs play a therapeutic role because of their anti-inflammatory and antioxidant properties and via inhibiting pyroptosis. (A) The antioxidant effect of the ADSCs in FB was studied by flow cytometry. Statistics analysis was performed using one-way ANOVA. *$P < 0.05$.(B) Immunoblots for expression of antioxidant protein SOD2 in FB cells, values are expressed as mean ± SD, statistics analysis was performed using one-way ANOVA, ***$P < 0.001$. (C) Senescence β-galactosidase staining in fibroblasts. (D) Immunoblots for expression of pyroptosis protein NLRP3, N-GSDMD, IL-β, caspase-1 and cleaved-caspase-1 p20 in J774A.1, values are expressed as mean ± SD and statistical analysis was performed using one-way ANOVA, ***$P < 0.001$. (E) Representative CLSM images of J774A.1 cells induced pyroptosis and co-cultured with ADSCs; cells were stained by ASC (red), NLRP3 (green), and nuclei (blue). Scale bar: 25 μm. (F–G) The proportion of FAM-FLICA caspase-1 (YVAD) (+) group of J774A.1 cells co-cultured with ADSCs was studied by flow cytometry, and statistical analysis was performed using one-way ANOVA, *$P < 0.05$. (H) Caspase-1 activity assay was studied by the absorbance of pNA at 405 nm; statistical analysis was performed using one-way ANOVA, ***$P < 0.001$. (I) LDH activity was studied by the absorbance at 490 nm; statistical analysis was performed using one-way ANOVA, ***$P < 0.001$. (J) Representative CLSM images of J774A.1 cells induced pyroptosis and co-cultured with ADSCs, cells were stained by caspase-1 (green) and nuclei (blue). Scale bar: 25 μm. (K) Immunoblots for expression of ECM proteins, COL1A1, COL3A1, MMP1, MMP9 and TIMP1 in FB cells, values are expressed as mean ± SD, statistical analysis was performed using one-way ANOVA, *P < 0.05, **P < 0.01, ***$P < 0.001$. (L) The study of macrophages releasing inflammatory cytokines by ELISA, values are expressed as mean ± SD and statistical analysis was performed using one-way ANOVA, *$P < 0.05$, **$P < 0.01$, ***$P < 0.001$. (M – N) The study of ADSCs to induce polarization in macrophages as detected by the surface markers M1 (CD86), M2 (CD163, CD206 double staining) by flow cytometry, statistical analysis was performed using one-way ANOVA, *$P < 0.05$, **$P < 0.01$, ***$P < 0.001$. (O) Immunoblots for expression of macrophage cell marker protein M1 (iNOS) and M2 (Arg-1), values are expressed as mean ± SD, statistical analysis was performed using one-way ANOVA, *$P < 0.05$, **$P < 0.01$, ***$P < 0.001$.

4.5. The characterization of hydrogels

The TSPBA linker was synthesized through a quaternization reaction between TMPA and 4-(bromomethyl) phenylboronic acid (Scheme S1), as verified by the 1H NMR (Figure S1)·1H NMR (400 MHz, D2O, δ): 7.90 (d, 4H), 7.61 (d, 4H), 4.62 (s, 4H), 3.42 (t, 4H), 3.15 (s, 6H), 2.46 (m, 2H).

Fig. 4A shows the synthetic route of the TPC Gel for the loading of ADSCs. The ROS-responsive TPC Gel is fabricated via borate ester bond formed between TSPBA and PVA, and the addition of collagen facilitated the formation of interpenetrating networks. Because high concentration of TSPBA may result in fast formation of hydrogels, which is unfavorable for the loading of ADSCs, the TPC Gel is prepared by mixing of PVA 1788 (8 wt %), TSPBA (10 wt %) and collagen (2 mg/mL) with the volume ratio of 5:2:3 (carmine was added for observation). As a control group, the TP Gel is prepared by using deionized water to replace collagen. Fig. 4B shows the gelation properties of TP Gel and TPC Gel, respectively. We also notice that the gelation of TPC requires approximately 50 min, which is slower than the TP Gel, suggesting the addition of collagen into the system reduces the gelation rate.

The microstructures of lyophilized PVA, TP Gel and TPC Gel are characterized by using SEM. Fig. 4C shows that the PVA forms both open cells and closed cells. However, the TP Gel forms closed cells, suggesting the crosslinking of PVA and TSPBA promotes the formation of hydrogels. More interestingly, the TPC Gel forms smaller and denser closed cells, suggesting that the addition of collagen contributed in the formation of interpenetrating networks.

Rheological scanning is carried out on TPC Gel by rheometer. Frequency scanning results (Fig. 4D) show that the storage modulus (G′) of Gel was higher than loss modulus (G″), suggesting the formation of hydrogels. In addition, the viscosity of the TPC Gel decreased with increasing shear frequency, showing the shear thinning property of TPC Gel. Because the shear frequency of 10 rad/s does not break the structure of Gel, the subsequent strain scanning is carried out in the same shear frequency. The strain scanning results (Fig. 4E) show that the G′-strain and G″-strain curves are in linear range from 0.1 % to 100 % in which the hydrogel structures are not damaged. However, when the strain is over 250 %, the G′-strain and G″-strain curves drop dramatically, suggesting that the hydrogel structures are damaged. Next, to examine the self-healing property, the TPC Gel was subjected to alternating strain scanning (Fig. 4F), and the 1-min scanning is performed alternately at 0.1 % and 350 % strain. The results show that G′ and G″ could return to approximately 75 % of their initial moduli, indicating that Gel is able to maintain hydrogel properties after injection. The injectability is demonstrated in Fig. 4G.

To test the response of the TP Gel and TPC Gel to the inflammatory reaction of damaged tissues, the scavenging of DPPH free radicals (0.1 mM) and H2O2 (20 mM) was demonstrated respectively. Fig. 4H and I shows that Gel is able to scavenge 80 % of DPPH free radicals within 6 h, and scavenge 99.9 % of H2O2 within 15 min. These results show excellent free radical scavenging capability of the Gel in pelvic floor repairing.

4.6. The hydrogels have excellent biocompatibility and antioxidant capacity

We investigated the biocompatibility and ROS scavenging ability of hydrogels. First, we evenly spread the hydrogels on the petri dish, and ADSCs were selected for co-culturing over a period of time. Staining of EdU, ki67, and live and dead cells revealed that ADSCs could grow in the hydrogel environment, having good proliferation ability (Fig. 5A, B, and C), ki67 expression was statistically different. CCK8 detection revealed that ADSCs had good cell viability in the hydrogel (Fig. 5E). Consequently, we examined the ability of hydrogels to scavenge ROS (the Gel/ADSCs group was co-cultured with hydrogels, ADSCs and macrophages). The results demonstrated that the Gel/ADSCs group was more effective at scavenging ROS (Fig. 5F and G). Thus, it was conjectured that hydrogels might provide adequate protection for ADSCs following implantation (see Fig. 6).

4.7. Hydrogel-delivered ADSCs can protect stem cells and exert subsequent therapeutic effects

We verified the cell protective effect of hydrogels following the cell implantation. Different groups of luc-GFP-ADSCs were injected into the vaginal wall of model rats, and regular imaging observations were conducted. As indicated by the results, in the Col/ADSCs group, only a small amount of ADSCs survived two weeks after surgery, and fluorescence was undetectable three weeks following surgery. In the Gel/ADSCs group, ADSCs remained viable three weeks following injection (Fig. 5J and K). Meanwhile, analysis of the frozen section exposed that cell masses were visible in the Gel/ADSCs group two weeks after injection and four weeks later, cells were found dispersed throughout the vaginal wall. A small number of ADSCs were detected in the Col/ADSCs group two weeks after injection, and none remained alive four weeks later (Fig. 5H and I).

5. Discussion

Presently, rodents are the most commonly used animal models for prolapse and urinary incontinence research [27]. The gross connective tissue anatomy of the pelvis of rodents is comparable to that of humans. Regarding structure and function, rodents are the preferred models for evaluating connective tissue formation in humans [28]. The ECM in the lamina propria and the surrounding connective tissue of the rat's vaginal wall are the most important components of the supporting structure. They are the direct force components in mechanical injury and can better simulate and restore mechanical injury during pregnancy and

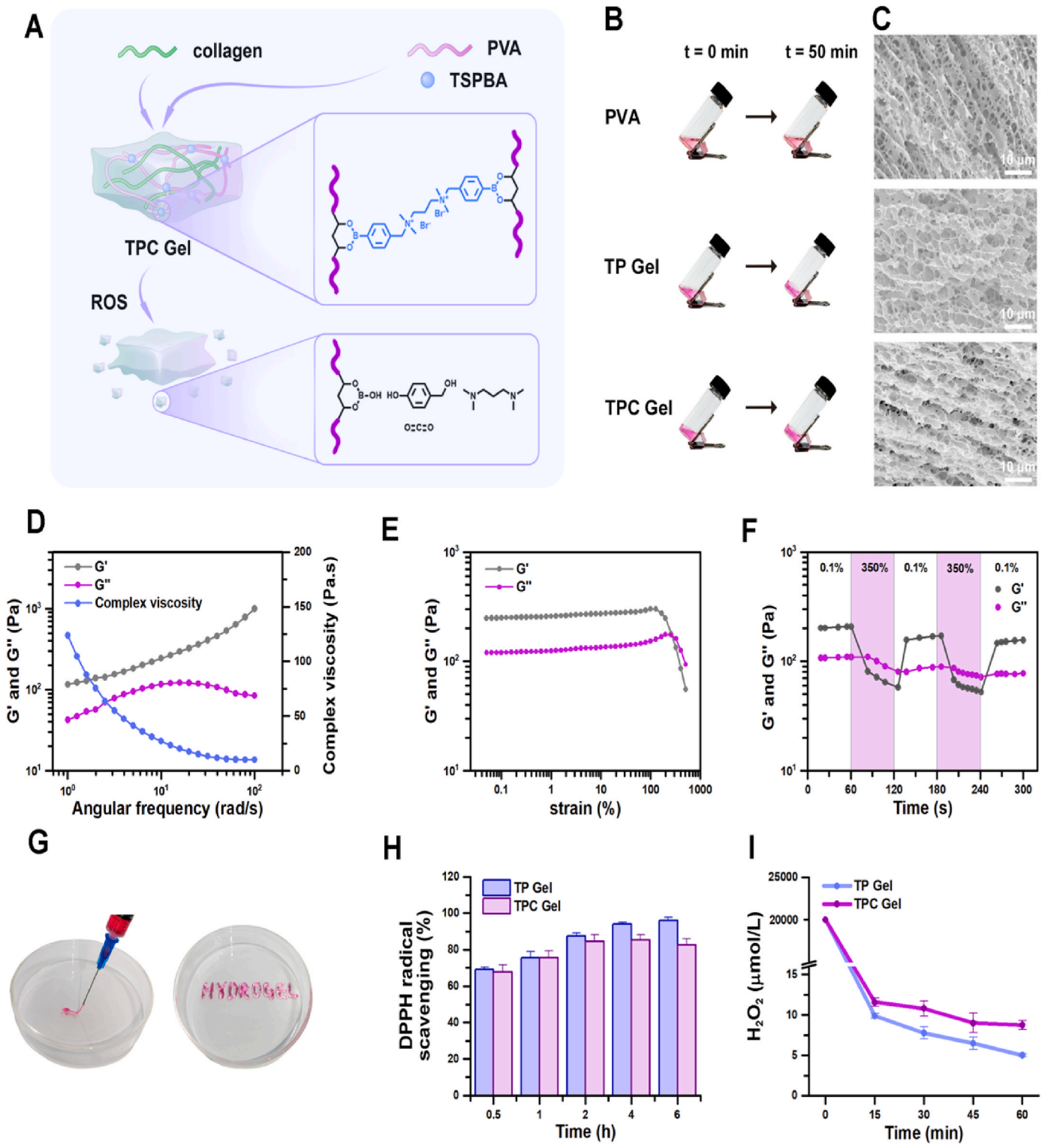

Fig. 4. Characterization of hydrogels. (A) Schematic illustration for the fabrication of ROS-responsive hydrogels. (B) Photographs and (C) SEM images of PVA, TP Gel, and TPC Gel, respectively (scale bars: 10 μm). (D–F) Rheological scanning of TPC Gel by rheometer: (D) Frequency scanning; (E) Strain scanning; (F) Alternative strain scanning. (G) Photographs for the injectability of TPC Gel. (H) Scavenging of DPPH free radicals and (I) H2O2 by TP Gel and TPC Gel.

delivery [29]. This study constructed a rat vaginal dilation model to simulate acute mechanical injury during pregnancy and delivery, and the distal pull was used to induce physiological dystocia to explore the possible key pathogenesis through molecular biology technology.

5.1. *The antioxidant capacity of stem cells plays a key therapeutic role*

Evidence suggests that MSC-based cell and decellularization therapy effectively reduces tissue damage and promotes tissue regeneration and repair, including pelvic floor tissue damage [30–33]. They contribute to maintaining stem cell activity and tissue homeostasis [34]. Numerous

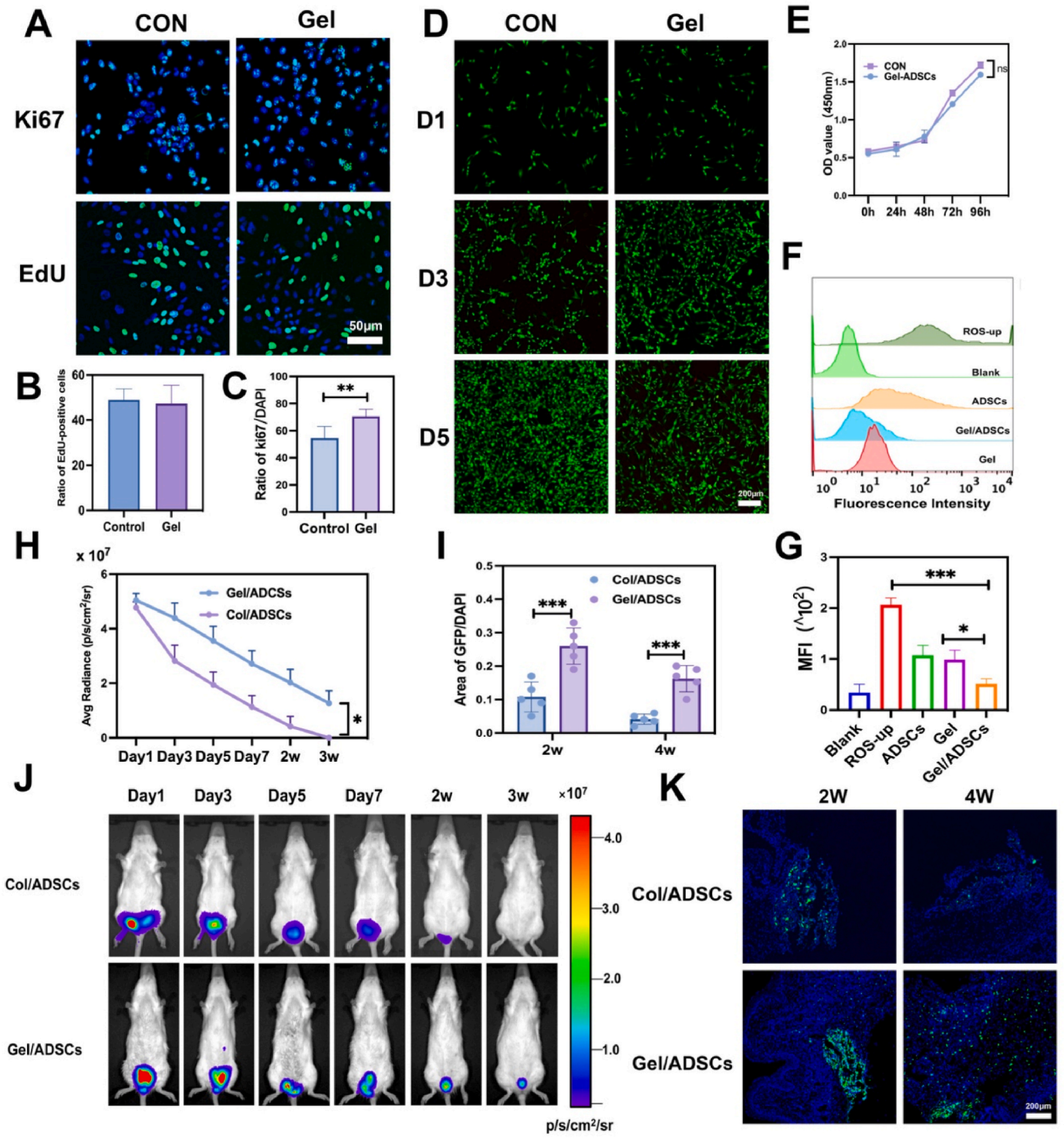

Fig. 5. Hydrogels have good biocompatibility, ROS scavenging and cell-carrying abilities.(A) EdU staining and ki67 fluorescence imaging of ADSCs co-cultured with plates and Gel. (B) EdU-positive cell proportion in ADSCs co-cultured with plates and Gel. (C) The ratio of semi-quantitative fluorescence imaging showing ki67 positive cell proportion in ADSCs co-cultured with plates and Gel. (D) Live-dead staining of ADSCs co-cultured with plates and Gel. (E) Viability of ADSCs co-cultured with Gel and plate. Data are shown as mean ± SD. (F–G) The ROS scavenging ability of Gel was studied by flow cytometry; statistical analysis was performed using one-way ANOVA, *$P < 0.05$, **$P < 0.01$, ***$P < 0.001$. (H–I) The fluorescence showed the distribution and number of ADSCs in rat vaginal wall tissue. Statistical analysis was performed by the unpaired *t*-test. ***$P < 0.001$. (J–K) The in vivo fluorescence imaging to visualize the bio-distribution in vivo at different time points following Col/ADSCs and Gel/ADSCs injection into the rats. Statistical analysis was performed by the unpaired *t*-test. *$P < 0.05$.

studies have demonstrated that the therapeutic properties of MSCs stem from their paracrine effects, which include immune regulation and tissue repair [35–37]. MSCs secrete growth factors, cytokines, chemokines, and extracellular vesicles (EVs), conferring the paracrine therapeutic ability to MSCs, leading to immune regulation and improvement of tissue damage [38]. However, the antioxidant capacity of stem cells has been discovered in recent years. ROS produced by oxidative stress is closely associated with cell damage and is involved in various

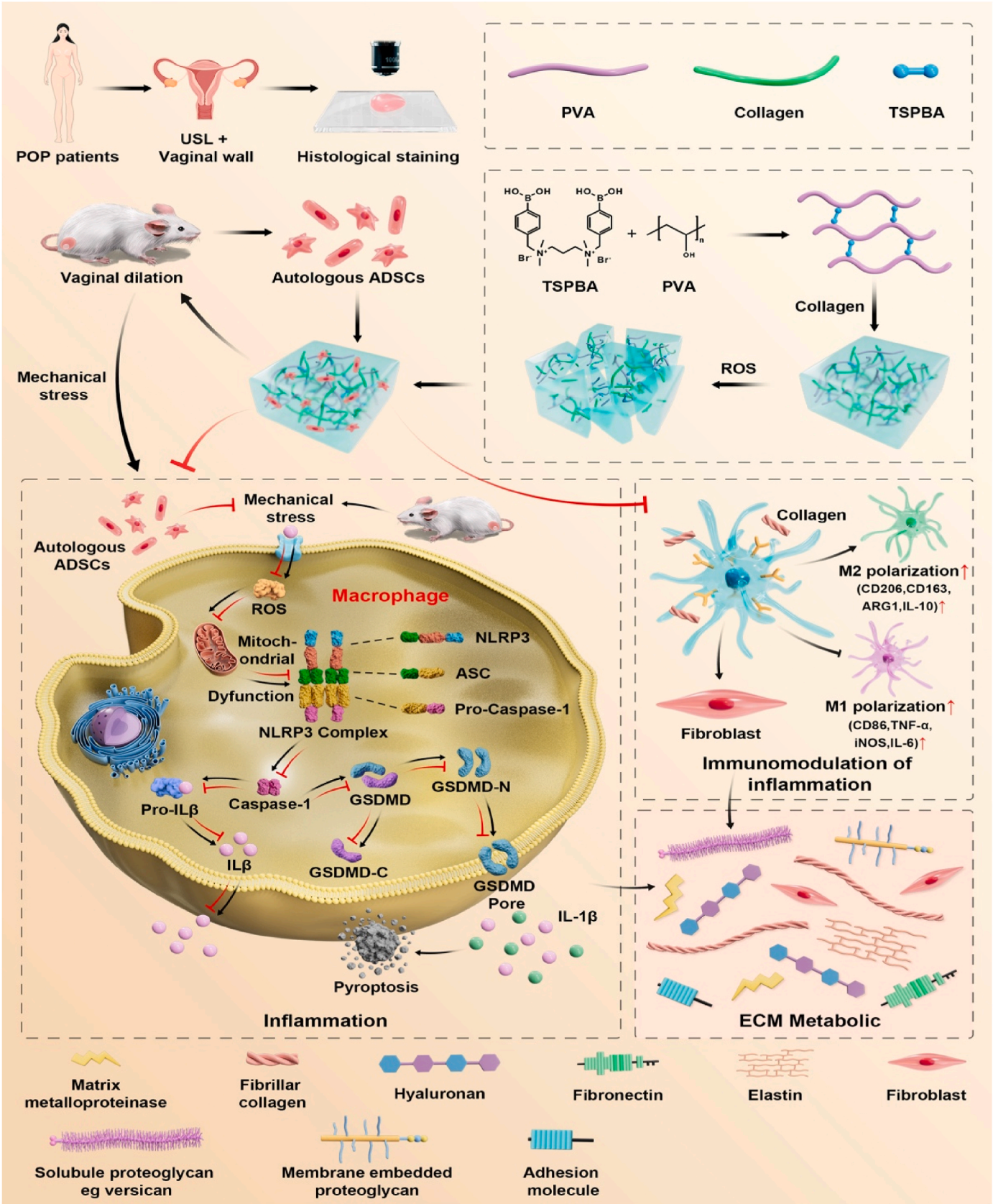

Fig. 6. A schematic showing the therapeutic effects of ADSCs on pelvic floor tissue damage caused by mechanical forces, and the preparation of ROS-responsive hydrogels for the treatment of the injury.

pathological processes [18,39,40]. This research also verified the positive therapeutic effect of ADSCs in reducing ROS accumulation after pelvic floor tissue and cell damage.

5.2. Pelvic floor tissue damage caused by mechanical force causes oxidative metabolism disorders

One of the initial causes of tissue damage and inflammatory response is mechanical force [41]. Pregnancy and vaginal delivery increase internal abdominal pressure, keeping the pelvic floor support structure in continuous load-bearing traction. Strong mechanical force may cause acute dilation, overstretch, or even fracture of the pelvic floor tissue during the second stage of labor, resulting in damage to pelvic floor tissue. The role of mechanical force injury in the pathogenesis of POP has been gradually uncovered in recent years [5,42–44]. Mechanical injury leads to oxidative stress in the pelvic floor support structure, causing ROS accumulation and ECM metabolic disorder. In this study, following mechanical injury, the vaginal wall of model rats exhibited ROS accumulation, demonstrating that mechanical damage can result in ROS production and buildup. Therefore, an imbalance of oxidative metabolism in pelvic floor tissue may be the primary cause of ECM metabolic disorder after mechanical injury, resulting in POP occurrence and development. The impact of oxidative stress injury on the function of pelvic floor tissue has not received sufficient consideration, available related reports are few, and its role and mechanism in pelvic floor injury have not been fully clarified. During vaginal delivery, mechanical compression of the pelvic tissues, tissue ischemia and hypoxia injury may exacerbate local oxidative stress. Furthermore, a large number of oxidative intermediates may cause damage to cells and tissues during vaginal delivery, resulting in the repair of pelvic floor tissues, which may be the key link and initiating factor of the onset of POP.

5.3. ROS accumulation induced by mechanical injury activates pyroptosis of macrophages, causing an imbalance of the immune microenvironment of pelvic floor tissues, leading to persistent chronic inflammation and aggravating pelvic floor support tissue damage

ROS can encourage the polarization of macrophages to the M1 type, and ROS accumulation is the key factor in activating macrophages to produce inflammatory bodies. Pyroptosis is a novel mode of cell death induced by NLRP3-containing inflammatory bodies, a programmed cell death like apoptosis, programmed necrosis and autophagy. Pyroptosis is a double-edged sword. On the one hand, mild pyroptosis is advantageous for maintaining cell homeostasis, enhancing immune function, and removing damage and pathogens to protect the host [45]. On the other hand, after pyroptosis, excessive inflammation is unconducive to the polarization of M1 macrophages to the M2 type, which promotes tissue repair, ultimately leading to the imbalance of the immune microenvironment and exacerbating disease progression [46]. The accumulation of ROS caused by oxidative stress disorder activates the pyroptosis signaling pathway, NLRP3/caspase-1, averting polarization of macrophages and ultimately resulting in immune microenvironment imbalance. Seldom study or mechanism of mechanical stress-induced pelvic floor support tissue injury has been reported.

According to recent research, ECM is now regarded as a highly dynamic partner of the immune system, providing structural support for the normal physiological activities of tissue cells and playing an indispensable role in immune regulation with its rich protein components and immunoactivity molecules in homeostasis and pathological states of the body [47]. On the contrary, the immune system can maintain stromal microenvironment homeostasis and repair stromal integrity after injury. ECM and immune cells are interdependent. ECM components offer dynamic tissue integrity, participate in and drive many biological reactions as signaling molecules, and their disorders are the direct or indirect causes of most chronic diseases [48]. ECMs aid immune cells in determining their final location and regulate their survival and function. Inflammation, tissue damage, and infection alter the chemical composition and mechanical properties of ECMs, which in turn cascade through many immune processes. The two mutually influence and dynamically regulate each other to maintain the body's homeostasis [19,49,50]. The results of our transcriptome sequencing indicated that immune-inflammatory disorder is a key contributor to pelvic floor tissue injury following mechanical trauma, and impeding tissue repair, macrophage inflammatory signal transduction, and inflammatory factors release could reduce ECM synthesis. Therefore, this study found a mechanical-immune-inflammation-tissue damage linkage.

5.4. Stem cells play an important role in reducing ROS production in pelvic floor tissue, thus regulating the immune microenvironment at the damaged site and promoting damage repair

Current research on the stem cells repair mechanism against POP is limited, and the antioxidant capacity of stem cells could be a factor in treating POP injury. As stated by the literature, MSCs can reduce ROS production, improve the antioxidant capacity of cells and tissues, decrease cellular response to inflammation and oxidation [20], and diminish inflammatory factors at the injured site, thus, protecting and repairing damaged tissues. Based on our previous results, stem cells can reduce inflammatory cytokines released by damaged fibroblasts. Therefore, it was theorized that stem cells exert their antioxidant capacity immediately following implantation at the injured site by lowering ROS accumulation in pelvic floor tissue, blocking the NLRP3/caspase-1 signaling pathway, and reducing IL-1β release and pyroptosis. In addition, they decrease the production of inflammatory factors and increase the expression of antioxidant-related proteins at the site of treatment.

The ability of stem cells to regulate the immune system also plays an important role in POP treatment [51]. Macrophages are crucial for inflammation, host defense, tissue repair, and metabolism [52]. Under the influence of tissue microenvironment signals, the M1 and M2 phenotypes of macrophages display a high degree of plasticity and dynamics and can transform into each other. Therefore, macrophages are in a continuous transition from M1 to M2 in tissues, and the different proportions of the two could indicate the direction of tissue inflammation, healing and remodeling [53]. The highly complex plasticity of macrophages is a host protective mechanism to maintain tissue stability during various stages of trauma and inflammation. Whether this effect is positive or negative depends on the polarization state of macrophages and the transformation and balance between M1/M2. M2 has potent anti-inflammatory properties and the ability to repair and regenerate. Moreover, M2 macrophages secrete VEGF, TGF-β and arginine, thereby increasing ECM synthesis, such as collagen and polyamine proteoglycans, and promoting tissue regeneration [54]. It has been reported that M2-type macrophages improve tissue damage by inhibiting the NLRP3 inflammasome signaling pathway [55], a rapid and effective transformation of pro-inflammatory M1-type macrophages at the injured site to anti-inflammatory M2-type macrophages may be more conducive to promoting tissue repair and restoring function. The paracrine soluble factors of ADSCs, such as IL-4, are vital molecules in the interaction between stem cells and macrophages, especially the M1 to M2 phenotype polarization transfer. Our study also found that ADSCs could induce the polarization of macrophages from M1 to M2 in vivo and in vitro. Therefore, we postulated that polarizing M1-type macrophages into M2-type macrophages could reduce the release of pro-inflammatory factors and cell pyroptosis, thus restoring the metabolic balance of ECM and repairing pelvic floor support structures.

5.5. Hydrogels can reduce ROS accumulation and load ADSCs well

In this study, we formulated an injectable ROS-responsive PVA@-COLI collagen complex hydrogel, which could regulate the oxidation imbalance environment at the damaged site. The hydrogel delivers a

better extracellular environment and biocompatibility for stem cells through ROS response clearance and collagen adhesion than the conventional local injection of ADSCs suspension, thus promoting a synergistic effect. On the one hand, ROS responsiveness can eliminate a substantial amount of ROS at the implant site. As ROS gradually decreases, so do hydrogels, and ADSCs are released to exert the ROS scavenging ability and subsequent therapeutic effect. On the other hand, ADSCs released at the site of injury exert paracrine repair and regulation of tissue damage. The hydrogel in this study could effectively prevent disease progression by restoring a healthy microenvironment in the damaged pelvic floor tissue. Moreover, it can collaborate with stem cells to enhance their therapeutic efficacy, reducing local inflammation/oxidative stress, increasing the protective barrier of cells to resist various stressors from the implant site, and increasing the attachment, survival and immune regulation ability of stem cells. Compared to local injections of single-cell suspension, it has multiple advantages, such as efficacy and safety.

This preliminary study demonstrates the potential of utilizing ROS responsive PVA/ColI hydrogel in combination with stem cells to treat pelvic floor injuries. However, further research is needed to advance this approach. In future studies, we will focus on developing new models and designs for pelvic floor injury repair that can be better adapted to different types of tissue injuries. In addition, we will work on enhancing hydrogel materials, improving stem cell loading strategies, and aligning material characteristics with the requirements of the repair microenvironment to improve the repair of tissue injuries. In addition, potential molecular mechanisms for the combined application of hydrogel systems and stem cells will be elucidated. Finally, it is important to note that there is a need to prolong the assessment of repair efficacy.

6. Conclusion

The mechanical force causes damage to the pelvic floor support structure, and poor repair plays a crucial role in the POP onset. Based on the study's in vivo and in vitro experimental verification results and literature reports, ROS accumulation was induced by mechanical force injury, activating NLRP3 inflammatory bodies and pyroptosis of macrophages, resulting in pelvic floor immune microenvironment and ECM metabolic disorders and poor repair of supporting structures. It may be the main pathogenesis of POP after acute mechanical injury. First, following acute mechanical injury, oxidative stress metabolism of pelvic floor tissues is misregulated, and a large number of ROS accumulates. Meanwhile, macrophages are rapidly gathered at the site of the injury. ROS can stimulate M1 macrophages to release NLRP3 inflammatories, induce IL-1β release and pyroptosis, and exacerbate the inflammation of damaged tissues. Consequently, chronic inflammation of fibroblasts in supporting tissues persists, impeding their migration, adhesion, and activities, inducing cell apoptosis, thereby affecting the metabolic balance of pelvic floor ECM collagen fibers, hindering the repair process, and preventing new collagen from shaping and functioning, thus leading to the disease occurrence. There are currently few reports on the effect of stem cells on mechanical pelvic floor injury, and the underlying mechanism is unknown. On the basis of our previous research findings and published literature, we hypothesized that stem cells could, on the one hand, use their antioxidant capacity to reduce the ROS accumulation in pelvic floor tissue and thus reduce pyroptosis to play a therapeutic role; on the other hand, they could have an immunoregulatory role to stimulate M1-type macrophages to polarized to M2-type macrophages, reducing the release of pro-inflammatory factors, and make remodeling towards tissue reconstruction. Moreover, stem cells release growth factors such as fibroblast growth factor, to stimulate collagen synthesis in damaged tissues, thereby facilitating the repair and regeneration of damaged tissues. We constructed PVA@COLI, ROS-responsive stem cell hydrogel, to overcome the low survival rate and poor therapeutic effect of cells injected directly with stem cells. The shell functions as a protective cell barrier to resist various environmental stressors and maintain cell activity. Reshaping the inflammatory microenvironment: ROS clearance properties of the hydrogel could reduce damage and reshape the site of inflammatory injury. It could be a promising tissue repair and regeneration method under the inflammatory environment of pelvic floor tissue injury.

CRediT authorship contribution statement

Xiaotong Wu: Conceptualization, Data curation, Formal analysis. **Fengshi Zhang:** Conceptualization, Data curation, Writing - original draft, Writing - review & editing. **Xiaolin Mao:** Investigation, Methodology. **Fujian Xu:** Methodology. **Xiaokang Ding:** Methodology, Supervision. **Xiuli Sun:** Funding acquisition, Supervision. **Jianliu Wang:** Project administration, Supervision.

Declaration of competing interest

The authors declare that they have no known competing financial interests or personal relationships that could have appeared to influence the work reported in this paper.

Data availability

Data will be made available on request.

Acknowledgements

This work was supported by the National Key Research and Development Program, China [2023YFC2411204, 2023YFC2411203]; National Natural Science Foundation, China [82301830, 82171615]; Peking University People's Hospital Scientific Research Development Funds, China [RDJP2022-51, RDGS2022-12]. All authors would like to thank Peking University People's Hospital Biobank (Beijing, China) for clinical specimens support.

Appendix A. Supplementary data

Supplementary data to this article can be found online at https://doi.org/10.1016/j.mtbio.2023.100910.

References

[1] J.L. Blomquist, A. Muñoz, M. Carroll, V.L. Handa, Association of delivery mode with pelvic floor disorders after childbirth, JAMA 320 (2018) 2438–2447.
[2] N.K. Mattsson, P.K. Karjalainen, A.M. Tolppanen, A.M. Heikkinen, H. Sintonen, P. Härkki, K. Nieminen, J. Jalkanen, Pelvic organ prolapse surgery and quality of life-a nationwide cohort study, Am. J. Obstet. Gynecol. 222 (2020) 588, e1-.e10.
[3] Z. Guler, J.P. Roovers, Role of fibroblasts and myofibroblasts on the pathogenesis and treatment of pelvic organ prolapse, Biomolecules 12 (2022).
[4] P. Petros, M.R. Beale, B. Abendstein, The mechanics and biomechanics of OASIS POP and incontinence-is active management of labour protective? Int Urogynecol J 31 (2020) 1727–1728.
[5] Y. Zhu, L. Li, T. Xie, T. Guo, L. Zhu, Z. Sun, Mechanical stress influences the morphology and function of human uterosacral ligament fibroblasts and activates the p38 MAPK pathway, Int Urogynecol J 33 (2022) 2203–2212.
[6] Y. Li, Q.Y. Zhang, B.F. Sun, Y. Ma, Y. Zhang, M. Wang, C. Ma, H. Shi, Z. Sun, J. Chen, Y.G. Yang, L. Zhu, Single-cell transcriptome profiling of the vaginal wall in women with severe anterior vaginal prolapse, Nat. Commun. 12 (2021) 87.
[7] R.D. Marcu, D.L.D. Mischianu, L. Iorga, C.C. Diaconu, M. Surcel, A.N. Munteanu, C. Constantin, G. Isvoranu, O.G. Bratu, Oxidative stress: a possible trigger for pelvic organ prolapse, J Immunol Res 2020 (2020), 3791934.
[8] K.M. Sheu, A. Hoffmann, Functional hallmarks of healthy macrophage responses: their regulatory basis and disease relevance, Annu. Rev. Immunol. 40 (2022) 295–321.
[9] S. Gordon, F.O. Martinez, Alternative activation of macrophages: mechanism and functions, Immunity 32 (2010) 593–604.
[10] J.M. Abais, M. Xia, Y. Zhang, K.M. Boini, P.L. Li, Redox regulation of NLRP3 inflammasomes: ROS as trigger or effector? Antioxidants Redox Signal. 22 (2015) 1111–1129.
[11] K.V. Swanson, M. Deng, J.P. Ting, The NLRP3 inflammasome: molecular activation and regulation to therapeutics, Nat. Rev. Immunol. 19 (2019) 477–489.
[12] Y. Zhang, F. He, Z. Chen, Q. Su, M. Yan, Q. Zhang, J. Tan, L. Qian, Y. Han, Melatonin modulates IL-1β-induced extracellular matrix remodeling in human

nucleus pulposus cells and attenuates rat intervertebral disc degeneration and inflammation, Aging (Albany NY) 11 (2019) 10499–10512.
[13] M.S.J. Mangan, E.J. Olhava, W.R. Roush, H.M. Seidel, G.D. Glick, E. Latz, Targeting the NLRP3 inflammasome in inflammatory diseases, Nat. Rev. Drug Discov. 17 (2018) 588–606.
[14] S. Emmerson, S. Mukherjee, J. Melendez-Munoz, F. Cousins, S.L. Edwards, P. Karjalainen, M. Ng, K.S. Tan, S. Darzi, K. Bhakoo, A. Rosamilia, J. A. Werkmeister, C.E. Gargett, Composite mesh design for delivery of autologous mesenchymal stem cells influences mesh integration, exposure and biocompatibility in an ovine model of pelvic organ prolapse, Biomaterials 225 (2019), 119495.
[15] S. Mukherjee, S. Darzi, K. Paul, J.A. Werkmeister, C.E. Gargett, Mesenchymal stem cell-based bioengineered constructs: foreign body response, cross-talk with macrophages and impact of biomaterial design strategies for pelvic floor disorders, Interface Focus 9 (2019), 20180089.
[16] H. Mizuno, M. Tobita, A.C. Uysal, Concise review: adipose-derived stem cells as a novel tool for future regenerative medicine, Stem Cell. 30 (2012) 804–810.
[17] H.M. Blau, G.Q. Daley, Stem cells in the treatment of disease, N. Engl. J. Med. 380 (2019) 1748–1760.
[18] R. Stavely, K. Nurgali, The emerging antioxidant paradigm of mesenchymal stem cell therapy, Stem Cells Transl Med 9 (2020) 985–1006.
[19] T. Wang, Z. Jian, A. Baskys, J. Yang, J. Li, H. Guo, Y. Hei, P. Xian, Z. He, Z. Li, N. Li, Q. Long, MSC-derived exosomes protect against oxidative stress-induced skin injury via adaptive regulation of the NRF2 defense system, Biomaterials 257 (2020), 120264.
[20] M. Zhao, S. Liu, C. Wang, Y. Wang, M. Wan, F. Liu, M. Gong, Y. Yuan, Y. Chen, J. Cheng, Y. Lu, J. Liu, Mesenchymal stem cell-derived extracellular vesicles attenuate mitochondrial damage and inflammation by stabilizing mitochondrial DNA, ACS Nano 15 (2021) 1519–1538.
[21] X. Wu, H. Guo, Y. Jia, Q. Wang, J. Wang, X. Sun, J. Wang, Adipose mesenchymal stem cell-based tissue engineering mesh with sustained bFGF release to enhance tissue repair, Biomater. Sci. 10 (2022) 3110–3121.
[22] X. Wu, Y. Jia, X. Sun, J. Wang, Acceleration of pelvic tissue generation by overexpression of basic fibroblast growth factor in stem cells, Connect. Tissue Res. 63 (2022) 256–268.
[23] J. Wang, Y. Ye, J. Yu, A.R. Kahkoska, X. Zhang, C. Wang, W. Sun, R.D. Corder, Z. Chen, S.A. Khan, J.B. Buse, Z. Gu, Core-shell microneedle gel for self-regulated insulin delivery, ACS Nano 12 (2018) 2466–2473.
[24] P. Yu, X. Zhang, N. Liu, L. Tang, C. Peng, X. Chen, Pyroptosis: mechanisms and diseases, Signal Transduct. Targeted Ther. 6 (2021) 128.
[25] X. Unamuno, J. Gómez-Ambrosi, B. Ramírez, A. Rodríguez, S. Becerril, V. Valentí, R. Moncada, C. Silva, J. Salvador, G. Frühbeck, V. Catalán, NLRP3 inflammasome blockade reduces adipose tissue inflammation and extracellular matrix remodeling, Cell. Mol. Immunol. 18 (2021) 1045–1057.
[26] I. Ali, A.A. Padhiar, T. Wang, L. He, M. Chen, S. Wu, Y. Zhou, G. Zhou, Stem cell-based therapeutic strategies for premature ovarian insufficiency and infertility: a focus on aging, Cells-Basel 11 (2022).
[27] F. Fang, Z. Zhao, J. Xiao, J. Wen, J. Wu, Y. Miao, Current practice in animal models for pelvic floor dysfunction, Int Urogynecol J 34 (2023) 797–808.
[28] P.A. Moalli, N.S. Howden, J.L. Lowder, J. Navarro, K.M. Debes, S.D. Abramowitch, S.L. Woo, A rat model to study the structural properties of the vagina and its supportive tissues, Am. J. Obstet. Gynecol. 192 (2005) 80–88.
[29] J.L. Lowder, K.M. Debes, D.K. Moon, N. Howden, S.D. Abramowitch, P.A. Moalli, Biomechanical adaptations of the rat vagina and supportive tissues in pregnancy to accommodate delivery, Obstet. Gynecol. 109 (2007) 136–143.
[30] V. Miceli, A. Bertani, Mesenchymal stromal/stem cells and their products as a therapeutic tool to advance lung transplantation, Cells-Basel 11 (2022).
[31] J. Wen, Z. Zhao, F. Fang, J. Xiao, L. Wang, J. Cheng, J. Wu, Y. Miao, Prussian blue nanoparticle-entrapped GelMA gels laden with mesenchymal stem cells as prospective biomaterials for pelvic floor tissue repair, Int. J. Mol. Sci. 24 (2023).
[32] G. Zito, V. Miceli, C. Carcione, R. Busà, M. Bulati, A. Gallo, G. Iannolo, D. Pagano, P.G. Conaldi, Human amnion-derived mesenchymal stromal/stem cells pre-conditioning inhibits inflammation and apoptosis of immune and parenchymal cells in an in vitro model of liver ischemia/reperfusion, Cells-Basel 11 (2022).
[33] O. Ben Menachem-Zidon, M. Gropp, B. Reubinoff, D. Shveiky, Mesenchymal stem cell transplantation improves biomechanical properties of vaginal tissue following full-thickness incision in aged rats, Stem Cell Rep. 17 (2022) 2565–2578.
[34] A. Keating, Mesenchymal stromal cells: new directions, Cell Stem Cell 10 (2012) 709–716.
[35] T.H. Chang, C.S. Wu, S.H. Chiou, C.H. Chang, H.J. Liao, Adipose-Derived stem cell exosomes as a novel anti-inflammatory agent and the current therapeutic targets for rheumatoid arthritis, Biomedicines 10 (2022).
[36] G. Kolios, V. Paspaliaris, Mesenchyme stem cell-derived conditioned medium as a potential therapeutic tool in idiopathic pulmonary fibrosis, Biomedicines 10 (2022).
[37] V. Miceli, M. Bulati, G. Iannolo, G. Zito, A. Gallo, P.G. Conaldi, Therapeutic properties of mesenchymal stromal/stem cells: the need of cell priming for cell-free therapies in regenerative medicine, Int. J. Mol. Sci. 22 (2021).
[38] G. Alberti, E. Russo, S. Corrao, R. Anzalone, P. Kruzliak, V. Miceli, P.G. Conaldi, F. Di Gaudio, G. La Rocca, Current perspectives on adult mesenchymal stromal cell-derived extracellular vesicles: biological features and clinical indications, Biomedicines 10 (2022).
[39] Y. Hou, W. Ding, P. Wu, C. Liu, L. Ding, J. Liu, X. Wang, Adipose-derived stem cells alleviate liver injury induced by type 1 diabetes mellitus by inhibiting mitochondrial stress and attenuating inflammation, Stem Cell Res. Ther. 13 (2022) 132.
[40] T. Jiang, S. Liu, Z. Wu, Q. Li, S. Ren, J. Chen, X. Xu, C. Wang, C. Lu, X. Yang, Z. Chen, ADSC-exo@MMP-PEG smart hydrogel promotes diabetic wound healing by optimizing cellular functions and relieving oxidative stress, Mater Today Bio 16 (2022), 100365.
[41] L.S. Fischer, S. Rangarajan, T. Sadhanasatish, C. Grashoff, Molecular force measurement with tension sensors, Annu. Rev. Biophys. 50 (2021) 595–616.
[42] N.T.H. Farr, S. Roman, J. Schäfer, A. Quade, D. Lester, V. Hearnden, S. MacNeil, C. Rodenburg, A novel characterisation approach to reveal the mechano-chemical effects of oxidation and dynamic distension on polypropylene surgical mesh, RSC Adv. 11 (2021) 34710–34723.
[43] G.L. Clark-Patterson, S. Roy, L. Desrosiers, L.R. Knoepp, A. Sen, K.S. Miller, Role of fibulin-5 insufficiency and prolapse progression on murine vaginal biomechanical function, Sci. Rep. 11 (2021), 20956.
[44] R. Uemura, D. Tachibana, M. Shiota, K. Yoshida, K. Kitada, A. Hamuro, T. Misugi, M. Koyama, Upregulation of PTK7 and β-catenin after vaginal mechanical dilatation: an examination of fibulin-5 knockout mice, Int Urogynecol J 32 (2021) 2993–2999.
[45] Z. Zhang, Y. Zhang, S. Xia, Q. Kong, S. Li, X. Liu, C. Junqueira, K.F. Meza-Sosa, T.M. Y. Mok, J. Ansara, S. Sengupta, Y. Yao, H. Wu, J. Lieberman, Gasdermin E suppresses tumour growth by activating anti-tumour immunity, Nature 579 (2020) 415–420.
[46] N. Li, J. Chen, C. Geng, X. Wang, Y. Wang, N. Sun, P. Wang, L. Han, Z. Li, H. Fan, S. Hou, Y. Gong, Myoglobin promotes macrophage polarization to M1 type and pyroptosis via the RIG-I/Caspase1/GSDMD signaling pathway in CS-AKI, Cell Death Dis. 8 (2022) 90.
[47] L. Sorokin, The impact of the extracellular matrix on inflammation, Nat. Rev. Immunol. 10 (2010) 712–723.
[48] R. Jayadev, M. Morais, J.M. Ellingford, S. Srinivasan, R.W. Naylor, C. Lawless, A. S. Li, J.F. Ingham, E. Hastie, Q. Chi, M. Fresquet, N.M. Koudis, H.B. Thomas, R. T. O'Keefe, E. Williams, A. Adamson, H.M. Stuart, S. Banka, D. Smedley, D. R. Sherwood, R. Lennon, A basement membrane discovery pipeline uncovers network complexity, regulators, and human disease associations, Sci. Adv. 8 (2022), eabn2265.
[49] A.J. Day, C.M. Milner, TSG-6: a multifunctional protein with anti-inflammatory and tissue-protective properties, Matrix Biol. 78–79 (2019) 60–83.
[50] T.E. Sutherland, D.P. Dyer, J.E. Allen, The extracellular matrix and the immune system: a mutually dependent relationship, Science 379 (2023), eabp8964.
[51] D. Lu, Y. Xu, Q. Liu, Q. Zhang, Mesenchymal stem cell-macrophage crosstalk and maintenance of inflammatory microenvironment homeostasis, Front. Cell Dev. Biol. 9 (2021), 681171.
[52] T.A. Wynn, K.M. Vannella, Macrophages in tissue repair, regeneration, and fibrosis, Immunity 44 (2016) 450–462.
[53] D. He, X. Kou, Q. Luo, R. Yang, D. Liu, X. Wang, Y. Song, H. Cao, M. Zeng, Y. Gan, Y. Zhou, Enhanced M1/M2 macrophage ratio promotes orthodontic root resorption, J. Dent. Res. 94 (2015) 129–139.
[54] Y. Chen, M. Guan, R. Ren, C. Gao, H. Cheng, Y. Li, B. Gao, Y. Wei, J. Fu, J. Sun, W. Xiong, Improved immunoregulation of ultra-low-dose silver nanoparticle-loaded TiO(2) nanotubes via M2 macrophage polarization by regulating GLUT1 and autophagy, Int. J. Nanomed. 15 (2020) 2011–2026.
[55] Y. Dai, S. Wang, S. Chang, D. Ren, S. Shali, C. Li, H. Yang, Z. Huang, J. Ge, M2 macrophage-derived exosomes carry microRNA-148a to alleviate myocardial ischemia/reperfusion injury via inhibiting TXNIP and the TLR4/NF-κB/NLRP3 inflammasome signaling pathway, J. Mol. Cell. Cardiol. 142 (2020) 65–79.